

Title	Probing interface defects in top-gated MoS2 transistors with impedance spectroscopy
Authors	Zhao, Peng;Azcatl, Angelica;Gomeniuk, Yuri Y.;Bolshakov, Pavel;Schmidt, Michael;McDonnell, Stephen J.;Hinkle, Christopher L.;Hurley, Paul K.;Wallace, Robert M.;Young, Chadwin D.
Publication date	2017-06-26
Original Citation	Zhao, P., Azcatl, A., Gomeniuk, Y. Y., Bolshakov, P., Schmidt, M., McDonnell, S. J., Hinkle, C. L., Hurley, P. K., Wallace, R. M. and Young, C. D. (2017) 'Probing Interface Defects in Top-Gated MoS2 Transistors with Impedance Spectroscopy', ACS Applied Materials & Interfaces, 9(28), pp. 24348-24356. doi: 10.1021/acsami.7b06204
Type of publication	Article (peer-reviewed)
Link to publisher's version	10.1021/acsami.7b06204
Rights	This document is the Accepted Manuscript version of a Published Work that appeared in final form in ACS Applied Materials & Interfaces, copyright © American Chemical Society after peer review and technical editing by the publisher. To access the final edited and published work see http://pubs.acs.org/doi/abs/10.1021/acsami.7b06204
Download date	2024-08-03 03:58:41
Item downloaded from	https://hdl.handle.net/10468/4682



UCC

University College Cork, Ireland
Coláiste na hOllscoile Corcaigh

Probing Interface Defects in Top-Gated MoS Transistors with Impedance Spectroscopy

Peng Zhao, Angelica Azcatl, Yuri Y Gomeniuk, Pavel Bolshakov, Michael Schmidt, Stephen J McDonnell, Christopher L Hinkle, Paul K. Hurley, Robert M. Wallace, and Chadwin Young

ACS Appl. Mater. Interfaces, **Just Accepted Manuscript** • DOI: 10.1021/acsami.7b06204 • Publication Date (Web): 26 Jun 2017

Downloaded from <http://pubs.acs.org> on July 3, 2017

Just Accepted

“Just Accepted” manuscripts have been peer-reviewed and accepted for publication. They are posted online prior to technical editing, formatting for publication and author proofing. The American Chemical Society provides “Just Accepted” as a free service to the research community to expedite the dissemination of scientific material as soon as possible after acceptance. “Just Accepted” manuscripts appear in full in PDF format accompanied by an HTML abstract. “Just Accepted” manuscripts have been fully peer reviewed, but should not be considered the official version of record. They are accessible to all readers and citable by the Digital Object Identifier (DOI®). “Just Accepted” is an optional service offered to authors. Therefore, the “Just Accepted” Web site may not include all articles that will be published in the journal. After a manuscript is technically edited and formatted, it will be removed from the “Just Accepted” Web site and published as an ASAP article. Note that technical editing may introduce minor changes to the manuscript text and/or graphics which could affect content, and all legal disclaimers and ethical guidelines that apply to the journal pertain. ACS cannot be held responsible for errors or consequences arising from the use of information contained in these “Just Accepted” manuscripts.

Probing Interface Defects in Top-Gated MoS₂ Transistors with Impedance Spectroscopy

Peng Zhao,¹ Angelica Azcatl,¹ Yuri Y. Gomeniuk,^{2,3} Pavel Bolshakov,¹ Michael Schmidt,² Stephen J. McDonnell,⁴ Christopher L. Hinkle,¹ Paul K. Hurley,² Robert M. Wallace,¹ and Chadwin D. Young^{*,1}

¹Department of Materials Science and Engineering, The University of Texas at Dallas, 800 W Campbell Rd, Richardson, TX 75080, USA

²Tyndall National Institute, Department of Chemistry, University of College Cork, Lee Maltings, Dyke Parade, Cork, Ireland

³V. Lashkaryov Institute of Semiconductor Physics, NAS of Ukraine, 41, pr. Nauki, Kyiv, Ukraine

⁴Department of Materials Science and Engineering, The University of Virginia, Charlottesville, VA, USA

Abstract The electronic properties of the HfO₂/MoS₂ interface were investigated using multi-frequency capacitance-voltage (C-V) and current-voltage characterization of top-gated MoS₂ metal-oxide-semiconductor field effect transistors (MOSFETs). The analysis was performed on few layer (5 - 10) MoS₂ MOSFETs fabricated using photolithographic patterning with 13 nm and 8 nm HfO₂ gate oxide layers formed by atomic layer deposition after in-situ UV-O₃ surface functionalization. The impedance response of the HfO₂/MoS₂ gate stack indicates the existence of specific defects at the interface, which exhibited either a frequency dependent distortion similar to conventional Si MOSFETs with unpassivated silicon dangling bonds, or a frequency dispersion over the entire voltage range corresponding to depletion of the HfO₂/MoS₂ surface,

1
2
3 consistent with interface traps distributed over a range of energy levels. The interface defects
4 density (D_{it}) was extracted from the C-V responses by the high-low frequency and the multiple-
5 frequency extraction methods, where a D_{it} peak value of $1.2 \times 10^{13} \text{ cm}^{-2} \text{ eV}^{-1}$ was extracted for a
6 device (7-L MoS₂ and 13 nm HfO₂) exhibiting a behavior approximating to a single trap
7 response. The MoS₂ MOSFET with 4-L MoS₂ and 8 nm HfO₂ gave D_{it} values ranging from
8 $2 \times 10^{11} \text{ cm}^{-2} \text{ eV}^{-1}$ to $2 \times 10^{13} \text{ cm}^{-2} \text{ eV}^{-1}$ across the energy range corresponding to depletion near the
9 HfO₂/MoS₂ interface. The gate current was below 10^{-7} A/cm^2 across the full bias sweep for both
10 samples indicating continuous HfO₂ films resulting from the combined UV ozone and HfO₂
11 deposition process. The results demonstrated that impedance spectroscopy applied to relatively
12 simple top-gated transistor test structures provides an approach to investigate electrically active
13 defects at the HfO₂/MoS₂ interface and should be applicable to alternative TMD materials,
14 surface treatments and gate oxides as an interface defect metrology tool in the development of
15 TMD-based MOSFETs.
16
17
18
19
20
21
22
23
24
25
26
27
28
29
30
31
32

33
34
35
36
37
38 **Keywords** Molybdenum disulfide (MoS₂), high-*k* dielectrics, interface defects, electrical
39 characterization, top-gated transistors, capacitance – voltage (C-V).
40
41
42
43
44
45

46 **Introduction**

47
48
49 Over the past decade, two-dimensional (2-D) materials have attracted considerable attention
50 due to their atomically-thin structure and their unique electronic, optical and mechanical
51 properties¹⁻³. Among these materials, transition metal dichalcogenides (TMDs) have
52 demonstrated satisfactory energy bandgap values and promising properties for future
53
54
55
56
57
58
59
60

1
2
3 applications in electronics and optoelectronics ⁴⁻¹⁷. Molybdenum disulfide (MoS₂), as the most
4 explored TMD material, has been reported to exhibit an electron mobility of 55 cm²/V·s in a
5 top-gated transistor with a single layer of MoS₂ ⁴⁻⁶, and a theoretical value of 410 cm²/V·s at
6 room temperature ⁷. Moreover, compared with monolayer MoS₂, few-layer MoS₂ has been
7 predicted and experimentally demonstrated as an excellent channel material to achieve high
8 mobility and reduced contact resistivity ⁸⁻¹². With the ultimate electrostatic control due to the 2-
9 D structure, an energy gap in the range of 1.2eV to 1.8eV, and the high mobility value, MoS₂ is
10 especially attractive for high performance, low power-consumption flexible electronics ^{1,10,18,19}.

11
12
13
14
15
16
17
18
19
20
21
22
23 As the utilization of high dielectric constant (high-*k*) gate oxide material in conventional
24 silicon CMOS processing has been demonstrated to reduce the gate leakage and enable further
25 scaling of transistors, high-*k* dielectrics are also considered extensively for TMD transistors
26 ^{5,10,11,16,18-28}. In addition, high-*k* materials can suppress the coulombic scattering in low
27 dimensional nanostructures, increasing the carrier mobility, as shown in the literature with both
28 theoretical simulation ²⁰ and experimental evidence ^{5,11}. Although back gated structures are ideal
29 for contact and doping research on TMD transistors ^{8,29,30}, top gate devices are more attractive
30 for integrated circuit manufacturing. Thus, investigating high-*k* deposition on TMDs and
31 understanding the interface properties is an important scientific and technological research area.

32
33
34
35
36
37
38
39
40
41
42
43
44
45 An obstacle of integrating high-*k* dielectrics on these 2-D materials is the lack of bonds
46 available at the surface that enables thin film deposition ^{21,22}. Many top-gated transistors in the
47 literature adopted thick gate dielectric deposition, usually from 15 nm to 50 nm ^{5,11,16,23}, to avoid
48 pin holes and non-uniformity in the dielectric. Recently, multiple surface functionalization
49 methodologies have been reported for thin, uniform high-*k* dielectric deposition on MoS₂ ^{22,24-27}.
50 Metal seed layers ²⁴, oxygen plasma treatment ^{22,25} and ultraviolet-ozone (UV-O₃) treatment ^{26,27}
51
52
53
54
55
56
57
58
59
60

1
2
3 are promising pre-deposition approaches to gain a uniform dielectric layer. However, since the
4 ultimate goal of these approaches is the enhancement of electronic device performance, detailed
5 reports on device performance related to the impacts of these treatments is vital, but only shown
6 in a few papers^{24,25,31}. Our previous research suggested that defects existed at the high-*k*/MoS₂
7 interface region after an ex-situ UV-O₃ treatment²⁸, but the gate oxide leakage on these large
8 area MOS structures affected the analysis, due to the rough surface of the bulk MoS₂ sample and
9 relatively large capacitor area. Recently, Azcatl et al.,^{26,27} reported that the non-destructive (i.e.,
10 no Mo-oxide formation) in-situ UV-O₃ treatment featured a uniform atomic layer deposited
11 (ALD) high-*k* oxide without unexpected interfacial layers for exfoliated MoS₂.
12
13
14
15
16
17
18
19
20
21
22
23
24

25 Impedance measurements are recognized as one of the fastest and most robust methods to
26 investigate properties of a dielectric and its interface with the underlying substrate. However,
27 impedance measurements of metal/high-*k* dielectric/TMD MOS system have only been reported
28 in a limited number of works^{10,11,18,31–33}. Most publications report capacitance - voltage (C-V)
29 curves without further analysis^{10,11,32}, or back-gated capacitors with high-*k* deposited on Si³³.
30 Recently, S. Park et al.³¹ reported C-V characteristics of capacitors with Al₂O₃ on 100-200 nm
31 thick MoS₂ yielding D_{it} values of $10^{11} \text{ cm}^{-2} \text{ eV}^{-1}$ to $10^{14} \text{ cm}^{-2} \text{ eV}^{-1}$. For high-*k* on chemical-vapor-
32 deposited (CVD) MoS₂ thin films, a comprehensive study of dielectric impedance was
33 performed, showing D_{it} extraction and modeling work based on capacitors with 30 nm ALD
34 HfO₂ on monolayer MoS₂ with 2nm Al as an interfacial seed layer¹⁸. Another relevant and useful
35 D_{it} extraction work has been reported by Takenaka et al.³³, which uses the Terman method to
36 analyze and compare interfaces of MoS₂ and SiO₂/HfO₂/Al₂O₃. The extracted D_{it} values are
37 about $1 \times 10^{13} \text{ cm}^{-2} \text{ eV}^{-1}$ regardless of the dielectric selection for back-gated devices on semi-bulk
38 MoS₂. However, the device architecture may not be commensurate with the necessary solution
39
40
41
42
43
44
45
46
47
48
49
50
51
52
53
54
55
56
57
58
59
60

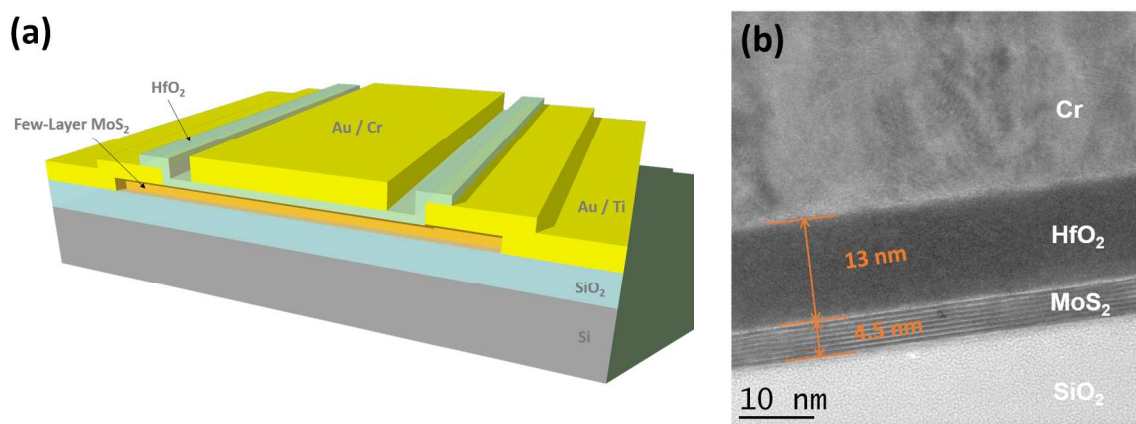
1
2
3 for continued device scaling where top-gated architectures dominate. Here, dielectric/substrate
4 interfaces are dependent upon how device fabrication was executed, and therefore, should be
5 investigated in this context.
6
7
8
9

10
11 In this work, we designed and fabricated top-gated transistors on exfoliated, few-layer MoS₂
12 as the test structures, with an in-situ UV-O₃ functionalization^{26,27} and 8 to 13 nm ALD HfO₂,
13 which are among the thinnest high-*k* dielectrics on top-gate TMD MOSFETs to date. As we use
14 photolithography for source/drain and gate patterning, the gated area is sufficiently large for C-V
15 characterization. Both transistor performance and gate-stack interface properties were
16 characterized, with an emphasis on the impedance spectroscopy of the dielectric. The interface
17 defect density (D_{it}) was extracted and analyzed by three different methods. Besides reporting the
18 interface properties of our transistors, the methodology can be potentially applied to other TMDs
19 and surface functionalization, beyond MoS₂ and UV-O₃ treatment.
20
21
22
23
24
25
26
27
28
29
30
31
32
33
34
35

36 **Experimental Methods**

37
38
39 The transistor structure used for the few-layer MoS₂ MOSFETs examined in this work is
40 shown in Fig. 1a. Before device fabrication, 270nm SiO₂ was thermally grown on highly doped
41 p-type Si wafers as a substrate. Few-layer MoS₂ flakes were mechanically exfoliated from
42 commercially available natural MoS₂ crystals and transferred onto the SiO₂. By using
43 conventional photolithography, we aligned a source/drain pattern on the photomask directly on
44 the selected flake. After patterning, Au/Ti (380/20nm) was deposited as contacts in an e-beam
45 evaporator at 2×10^{-6} Torr, followed by a lift-off process. Thereafter, a 15-minute in-situ UV-O₃
46 surface treatment²⁶ was performed. The UV-O₃ is generated based on irradiance from the fused
47
48
49
50
51
52
53
54
55
56
57
58
59
60

1
2
3 quartz envelope, low pressure UV Hg lamp employed previously^{26,27} and is estimated to be 5
4
5 mW/cm² which ensures no etching or Mo-oxide formation according to S. Park et al.³¹
6
7
8 Following the UV-O₃ surface preparation, HfO₂ was deposited at 200°C in the ALD chamber
9
10 immediately after the treatment without a break in vacuum. The thermal ALD used H₂O and
11
12 TDMA-Hf as the precursors, and started the deposition with a TDMA-Hf pulse. We intentionally
13
14 avoided annealing the HfO₂ after deposition to study the effects of the UV-O₃ functionalization
15
16 treatment and its role on HfO₂/MoS₂ interface properties without the impact of any subsequent
17
18 annealing. The final step of fabrication was patterning and evaporating of Au / Cr (250/50nm)
19
20 metal gate. The typical MoS₂ thickness studied in our work was about 5-10 layers (3-6 nm). The
21
22 device size was determined by both lithography and the flake shape. Electrical measurements in
23
24 this work were performed using a Keithley 4200 Semiconductor Characterization System and an
25
26 Agilent E4980A LCR meter at room temperature (25°C) in a shielded probe station.
27
28
29
30
31
32
33
34
35



51
52
53
54
55
56
57
58
59
60

Figure 1. (a) Schematic cross section of the top-gated MoS₂ field effect transistor structure used in this work. Gate stack: Au / Cr / HfO₂ / MoS₂. (b) Cross sectional transmission electron microscopic image of the metal/HfO₂/MoS₂ transistor gate stack. 13nm HfO₂ is uniformly deposited on a 7-layer MoS₂ flake, showing no evidence of unintentional oxidation of the MoS₂ surface.

Results and Discussion

A high-resolution transmission electron microscopic (TEM) image is shown in Fig.1b, illustrating the cross section of a device gate stack with 7 layer MoS₂ and a 13 nm HfO₂ dielectric. The active channel length under the metal gate is 6.5 μm and the channel width is 9.5 μm. Fig. 2a shows the I_{DS}-V_{GS} and the gate leakage characteristics for this MoS₂ transistor. V_{DS} was kept at 0.5V. An excellent on/off ratio of 10⁶ was observed, with an ultra-low leakage current on the gate. The MoS₂ was intrinsically n-type doped, consistent with our previous observation²⁸ and literature reports^{5,8,24,29}. The relatively large negative threshold voltage (V_T = -3V) is possibility due to the fixed positive charge in the dielectric layer(s). Similar large |V_T| was also observed by other researchers using top-gated MoS₂ transistors with high-*k* dielectrics^{11,24}. Since the HfO₂ is deposited at low temperature (200 °C) with no post deposition annealing (to assess the UV-O₃ treatment without convolution from additional annealing), a possible net oxide charge being present in the HfO₂ layer may result. Furthermore, possible contribution of induced charges in the underlying SiO₂ from potential x-rays exposure during the electron beam deposition process – which was used to form the metal gate and source/drain regions – could occur. Thus, both oxide layers could possess trapped charge. Assuming the threshold voltage shift ΔV=-3V originates from oxide charges, the density of the positive fixed charges can be estimated by $Q_f / q = - C_{ox} \cdot \Delta V / q = 1.4 \times 10^{13} / \text{cm}^2$. Fig. 2b shows the I_{DS}-V_{DS} curves with V_{GS} swept from -4 V to 0 V. A non-linear region was observed at low V_{DS}, likely because of high resistance Schottky barriers at the source/drain contacts associated with this unannealed device^{5,34}. This is expected, as there is no intentional doping in the MoS₂ film in the source and drain region. As is the case in conventional 3D semiconductors, increasing the doping

in the MoS₂ film to high concentrations ($> 1 \times 10^{19} \text{ cm}^{-3}$), for example via Nb doping³⁵, significantly reduces the specific contact resistivity at the Ti/MoS₂ interface. In addition, it is noted from Fig.1a that the top-gated MOSFET has non-gated regions between the gate edge and the source and drain contacts (approximately 1-2 μm on each side), which is another source of series resistance in the structure.

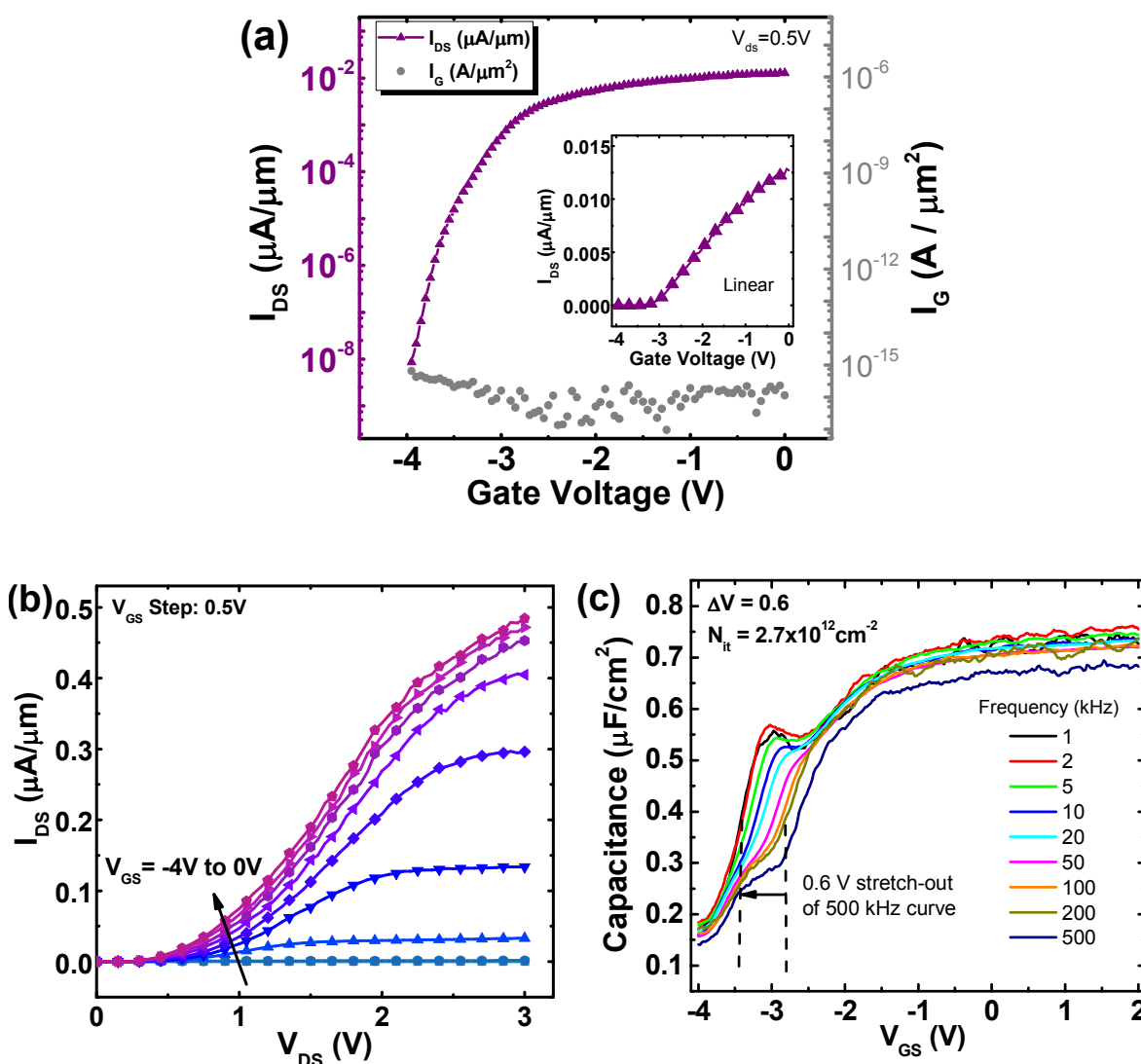
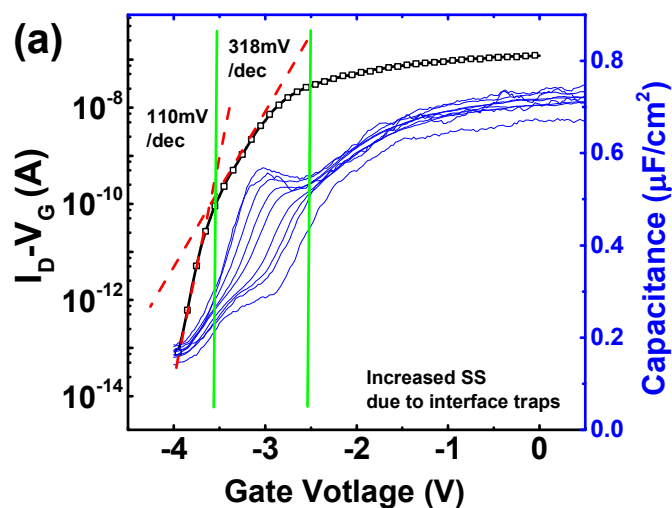
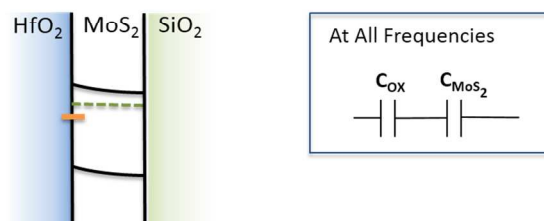


Figure 2. Electrical characterization of device with 13 nm HfO₂ and 7-layer MoS₂ (L=6.5 μm , W=9.5 μm). (a) I_{DS} - V_{GS} : $I_{ON}/I_{OFF} = 10^6$ with ultra-low gate leakage; (b) I_{DS} - V_{DS} with V_{GS} from -4 V to 0 V; (c) C-V: frequency

dependence, where a “hump” in the range -2.5 to -3.5 V is indicating an interface defect response. The 0.6 V stretch-out of 500 kHz curve indicates the Fermi energy pinning at MoS₂ / HfO₂ interface.



(b) (i) $V_{GS} > -2.8$ V in depletion region



(ii) -3.4 V $< V_{GS} < -2.8$ V (E_F pinned)

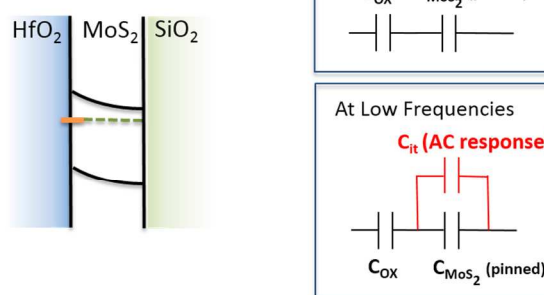


Figure 3. (a) I_D - V_G and multi-frequency C-V overlaid to illustrate the impact of D_{it} in both measurements occurs at the same V_g . SS is degraded due to interface traps and $D_{it} = 1.6 \times 10^{13} \text{ cm}^{-2} \text{ eV}^{-1}$ is estimated. (b) Energy band diagram of high- k / MoS₂ interface and equivalent circuits. (i) At gate voltages higher than -2.8 V or lower than -3.4

1
2
3 V, the total AC capacitance is due to the C_{ox} and C_{MoS_2} connected in series. (ii) At gate voltage between -3.4 V and -
4
5 2.8 V, the E_F is pinned at interface, and there is an AC response at low frequencies due to D_{it} but no AC response at
6
7 high frequencies.
8

9
10 To investigate the electronic properties at HfO_2/MoS_2 interface, the source and drain were
11
12 connected to one terminal of the LCR meter, while the gate is connected to the other terminal.
13
14 Variable frequency C-V measurements were conducted. The back gate contact was intentionally
15
16 floated to minimize the effect from oxide charge in the underlying SiO_2 . The frequency
17
18 dependence is shown in Fig. 2c. Since this transistor operates in accumulation mode, the reaction
19
20 of the majority carriers (electrons) to the ac signal is observed. In contrast to our previous study
21
22 on the ex-situ UV- O_3 treatment and bulk MoS_2 crystals²⁸, these C-V frequency dependence
23
24 results showed a highly improved high- k/MoS_2 interface, with significantly less dispersion and
25
26 lower gate leakage due to the in-situ UV- O_3 treatment and the few-layer TMD thickness. The C-
27
28 V characteristics demonstrate an approximately constant capacitance for positive gate voltage,
29
30 corresponding to the HfO_2 gate oxide capacitance, and a decrease in capacitance in the region -
31
32 2V to -4 V, consistent with depletion of negative charge at the HfO_2/MoS_2 interface. It is noted
33
34 that the region of surface depletion in the C-V response in Fig. 2c, is consistent with the sub-
35
36 threshold region in the transfer characteristics in Fig. 2a. The measured accumulation
37
38 capacitance is $0.76\mu F/cm^2$. Based on cross section TEM images, the HfO_2 is 13nm, and assuming
39
40 a k value of 17 for ALD grown HfO_2 , this would yield a maximum capacitance value of
41
42 $1.1\mu F/cm^2$. The lower value obtained experimentally, suggests the possibility of a lower k value
43
44 interface transition region between the HfO_2 and the MoS_2 which is not immediately obvious
45
46 from the TEM analysis.
47
48
49
50
51
52
53
54
55
56
57
58
59
60

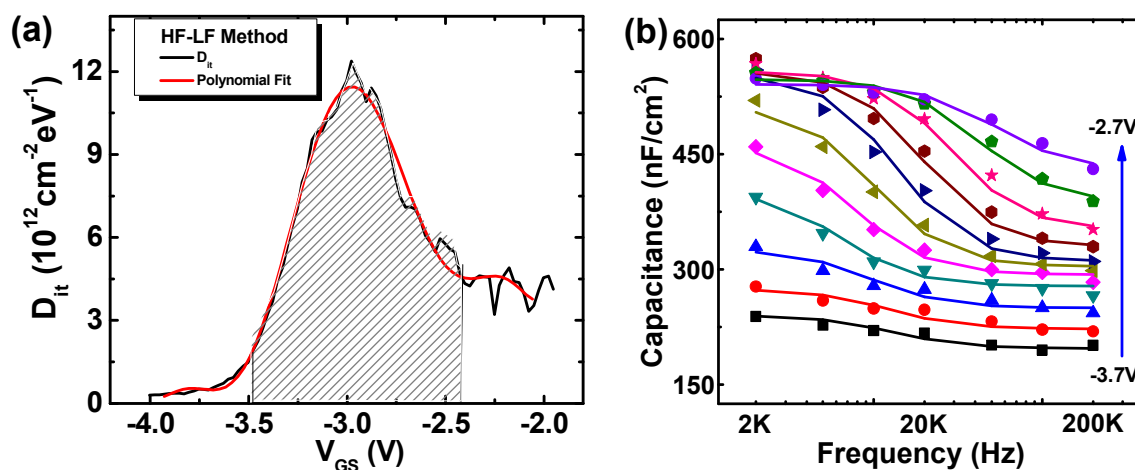
1
2
3 In the capacitance-voltage response in the region -4 V to -2 V, a frequency-dependent
4 distortion (“hump”) in the depletion region is observed, which is consistent with an electrically
5 activated trap response at the high- k /MoS₂ interface region. In conventional Si MOSFETs with
6 either SiO₂ or high- k oxides, this “hump” is usually attributed to interface traps which exhibit a
7 peak density at a specific energy in the bandgap^{36,37}, and usually a forming gas anneal around
8 400°C can passivate the defects^{38,39}, which are primarily silicon dangling bond (P_b) defects. The
9 C-V response of Si control sample under the same ALD condition was reported in our previous
10 work²⁸. HfO₂ formed at low temperature (200°C), without any higher temperature annealing in
11 N₂ or H₂/N₂ can exhibit gap states which result in C-V hysteresis, interface defect response, and
12 lower than expected dielectric constant. However, the HfO₂/Si control sample will not be
13 representative of the HfO₂/MoS₂ interface due to the different substrate material and interfacial
14 condition. (e.g. The Si substrate surface will spontaneously form a SiO₂-like interfacial layer
15 during an ALD process, which primarily determines the interfacial property of the HfO₂/Si⁴⁰).
16 Published C-V frequency dependence data on a metal / (30nm) HfO₂ / monolayer MoS₂ gate
17 stack was reported by Zhu et al.¹⁸, where chemical vapor deposited (CVD) MoS₂ was utilized in
18 the device structure. Compared with the device based on CVD MoS₂, this gate stack with
19 mechanically exfoliated MoS₂ shows much less frequency dispersion, suggesting significantly
20 fewer interface defects. A limited study of the C-V frequency dependence on semi-bulk MoS₂
21 with Al₂O₃ has also been reported³¹, where interface defects (D_{it}) ranging from 10¹¹ cm⁻²eV⁻¹ to
22 10¹⁴ cm⁻²eV⁻¹ were reported. However, the lateral shift of C-V curves possibly convoluted
23 positive oxide charge with interface defects in the D_{it} extraction process.
24
25
26
27
28
29
30
31
32
33
34
35
36
37
38
39
40
41
42
43
44
45
46
47
48
49
50
51
52

53 The techniques that we are about to describe to analyze the D_{it} are only valid when the device
54 is not fully depleted, which must be carefully adhered to when using very thin flakes. In this
55
56
57
58
59
60

1
2
3 work, the flake is not fully depleted over the bias range where the D_{it} response is detected. If the
4
5 MoS₂ thin film is fully depleted, the capacitance should be 0 F (or at a constant number over a
6
7 voltage range due to parasitic capacitance components)⁴¹. As shown in Fig. 3a, at about -3V
8
9 where interface traps are detected, the transistor is not fully turned off (i.e., not fully depleted and
10
11 still has carriers in the flake responding to the AC signal). Further evidence, based on series
12
13 resistance analysis (supporting information Fig. S1, S2), confirms that the device is not fully
14
15 depleted in the V_g range used to analyze the D_{it} from the multi-frequency C-V measurements.
16
17 Due to the influence of the interface traps, the inverse subthreshold slope (SS) also increases at
18
19 around -3V. This change of SS is also consistent with the charging of MoS₂/HfO₂ interface traps
20
21 providing an independent measurement technique indicating that the C-V response is detecting
22
23 interface traps at the corresponding region of the C-V response. SS can be used to roughly
24
25 estimate D_{it} since $SS = 60\text{mV} \cdot [1 + (C_{dm} + C_{it})/C_{ox}]$, where C_{dm} is the capacitance of depleted MoS₂
26
27 and C_{it} is the capacitance due to interface traps. Thus, C_{it} and D_{it} (C_{it}/q) can be estimated by
28
29 comparing the change in SS around -3.8 V (110 mV/dec) and around -3.2 V (318 mV/dec). The
30
31 calculated result gives $D_{it} = 1.6 \times 10^{13} \text{ cm}^{-2} \text{ eV}^{-1}$.
32
33
34
35
36
37
38

39
40 Next, we quantified the D_{it} from the C-V response (Fig. 2c). As the frequency is increased
41
42 from 1 kHz to 500 kHz, this reduces the AC response of the interface defects to the measured
43
44 capacitance, resulting in the dispersion of capacitance with frequency noted in the region from -
45
46 2.5 V to -3.5 V in Fig. 2c. In the limit of increasing frequency, the interface defects will only
47
48 respond to the DC bias (high frequency D_{it} response), and the interface states will be evident as a
49
50 “plateau” region of the C-V in the case where the interface states are located in a narrow band of
51
52 energies. From Fig. 2c, at frequencies above 100 kHz, an approximate plateau region is observed.
53
54 At 500 kHz this region extends from -2.8 V and -3.4 V. We interpret this 0.6V gate voltage
55
56
57
58
59
60

region to be due to the DC response of the defects⁴². This is illustrated in schematic energy band diagrams in Fig. 3b, with surface Fermi level pinning due to interface states with a peak density in a specific energy in the band gap⁽¹⁾. The total density of interface defects, in the areal density units of cm^{-2} , can be estimated from the oxide capacitance and the width of the plateau region in the 500kHz CV response, and this yields an interface trap density $D_{it} = 2.7 \times 10^{12} \text{ cm}^{-2}$. A more detailed calculation is shown in the supporting information S.3. Although the possibility that the defects still respond with AC signal at 500kHz could not be fully excluded, an abrupt C-V distortion due to peaked distribution of interface defects⁴² is consistent with our following D_{it} extraction and analysis.



⁽¹⁾ The plateau region is not a constant capacitance. This would only occur for a mono-energetic defect level at a temperature of zero K.

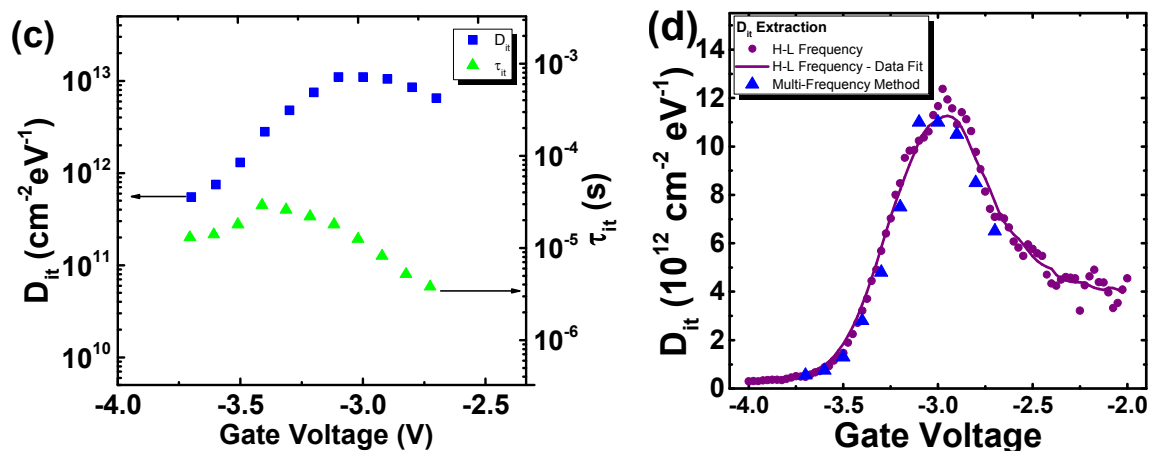


Figure 4. D_{it} extraction. (a) D_{it} vs V_{GS} , calculated by High-Low Frequency method; (b) Re-plotted “Capacitance vs Voltage” to “Capacitance vs Frequency” (dots), and modeling (solid lines); (c) D_{it} vs V_{GS} and τ_{it} vs V_{GS} , from the modeling work in (b); (d) Comparison of two D_{it} extraction methods in (a) and (c), showing similar D_{it} distribution, with a D_{it} peak at $1.2 \times 10^{13} \text{ cm}^{-2} \text{eV}^{-1}$.

Fig. 4a shows the D_{it} calculated by the conventional high-low frequency method⁴² from equations

$$C_{it} = \left(\frac{1}{C_{LF}} - \frac{1}{C_{ox}} \right)^{-1} - \left(\frac{1}{C_{HF}} - \frac{1}{C_{ox}} \right)^{-1} \quad (1)$$

$$D_{it} = C_{it}/q \quad (2)$$

where capacitance of interface traps (C_{it}) represents the capacitance when all the traps reacted with AC signal at low frequency; C_{LF} and C_{HF} are the capacitance measured at 1 kHz and 500 kHz respectively. In Fig. 4a, the polynomial function is a guide to the eye. D_{it} ranges from the order of 10^{12} to $10^{13} \text{ cm}^{-2} \text{eV}^{-1}$, with a peak value of $1.2 \times 10^{13} \text{ cm}^{-2} \text{eV}^{-1}$. The peak value is one order of magnitude lower than what was reported in reference³¹ using the same high-low frequency method, and aluminum oxide as the dielectric. It is in the same range as the defect density in literature for exfoliated MoS_2 by photo-excited charge collection spectroscopy⁴³. Translating each gate voltage in Fig. 4a to a corresponding surface potential at the $\text{MoS}_2/\text{HfO}_2$

1
2
3 interface, requires a known value of the active *n*-type doping concentration in the MoS₂. This
4
5 value is not readily known for the geological samples employed here, and as a consequence, the
6
7 D_{it} versus energy in the MoS₂ energy gap cannot be determined for these devices.
8
9

10
11 An alternative method was also employed to extract D_{it} ¹⁸. Instead of only using the C-V data
12
13 of high and low frequencies, data from the complete span of frequencies was used, and using this
14
15 approach both D_{it} and the trap time constant τ_{it} can be extracted. (The importance of τ_{it} is that one
16
17 can extract the trap cross section, σ , and trap energy, E_T , with temperature dependent
18
19 experiments³³ to understand the physical origin of the interface traps, and this is beyond the
20
21 scope of this work.) In this multi-frequency method, C_{it} is determined by D_{it} and τ_{it} at certain
22
23 voltages.
24
25

$$C_{it} = \frac{qD_{it}}{1+\omega^2\tau_{it}^2} \quad (3)$$

26
27
28
29
30

31 where $\omega=2\pi f$, and f is the applied AC frequency. Thus, at certain voltages, D_{it} and τ_{it} can be
32
33 extracted from the C-f or C- ω relationship. Fig. 4b shows the measured data (symbols) and
34
35 model fit (lines) for the capacitance versus frequency for the voltage range corresponding to the
36
37 interface defects response in the C-V characteristic. From Fig. 4b, the values of D_{it} , and the
38
39 corresponding τ_{it} values, can be determined at each gate voltage, and the characteristics are
40
41 shown in Fig. 4c. The two methods are compared in Fig. 4d, demonstrating consistency between
42
43 the two D_{it} extraction approaches. Detailed modeling work for these two methods can be found
44
45 in S.3 and S.4.
46
47
48
49
50
51
52
53
54
55
56
57
58
59
60

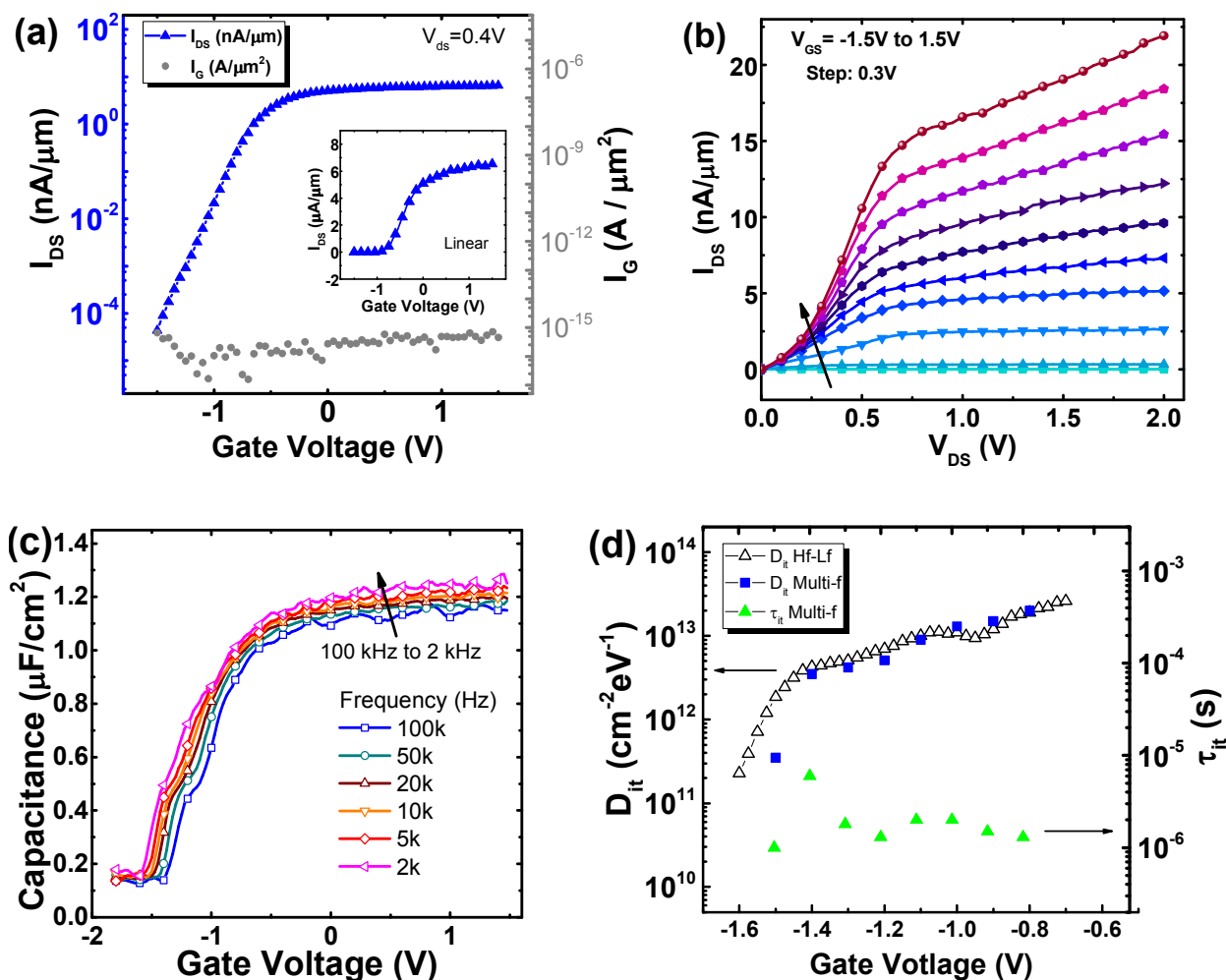


Figure 5. Electrical characterization and D_{it} extraction of a device with 8 nm HfO₂ and 4-layer MoS₂. ($W=7.2\mu\text{m}$, $L=5.6\mu\text{m}$) (a) I_{DS} - V_{GS} and gate leakage; (b) Corresponding I_{DS} - V_{DS} ; (c) C-V: frequency dependence; C-V curves disperse in the entire depletion voltage range, indicating interface traps in range of energy levels; (d) D_{it} vs V_{GS} and τ_{it} vs V_{GS} , D_{it} ranges from $2 \times 10^{11}\text{ cm}^{-2}\text{ eV}^{-1}$ to $2 \times 10^{13}\text{ cm}^{-2}\text{ eV}^{-1}$, with both H-L frequency method and multi-frequency method.

Due to possible variation in the electronic properties of exfoliated MoS₂ flakes for differing samples, and within a given crystal, in addition to contaminants and the presence of surface defects⁴⁴, we applied the same methods on a different MoS₂ transistor with 8nm HfO₂ and a 4-layer MoS₂ flake to verify if the C-V analysis method is more broadly applicable. Fig. 5a and 5b shows the I_{DS} - V_{GS} , gate leakage and I_{DS} - V_{DS} characteristics of this transistor. The gated area is

1
2
3 width \times length = 7.2 μm \times 5.6 μm . Fig. 5c and 5d shows the C-V frequency dependence, along
4
5 with the extracted D_{it} with two methods. The C-V frequency dispersion (Fig. 5c) suggests a
6
7 different distribution of interface defects at the $\text{HfO}_2/\text{MoS}_2$ interface compared to the sample
8
9 analyzed in Fig. 4. The frequency dependent C-V characteristics are consistent with an interface
10
11 state density distributed throughout the MoS_2 energy gap at the $\text{HfO}_2/\text{MoS}_2$ interface. Fig. 5d
12
13 shows the D_{it} and τ_{it} extracted using high-low frequency and multi-frequency methods. The
14
15 magnitude of D_{it} and τ_{it} are comparable to the 7-layer MoS_2 flake MOSFET shown in Fig. 4, but
16
17 in this case no peak in D_{it} is evident. Similar variation has also been reported in other
18
19 publications using thicker MoS_2 layers³³, and the variation from sample to sample (with
20
21 nominally identical processing) is also manifest in the transport properties³². This variability in
22
23 interface and transport properties is most likely a consequence of the high density and variability
24
25 of impurities and defects in both geological and grown MoS_2 .^{44,45}
26
27
28
29
30
31

32 Interfacial sulfur vacancies^{46,47} and other types of surface structural defects⁴⁸ are the defects
33
34 often observed by researchers, and can potentially generate these defect responses in the
35
36 impedance measurement. One possible suggestion for the defect level which shows a peak
37
38 response at a specific energy in the band gap (Fig. 4), is that the defect results from sulfur
39
40 vacancies³³, which is reported to have an energy level of 0.35eV from mid gap, from
41
42 measurements⁴⁶. The alternative behavior of an almost constant D_{it} across the energy gap (Fig.
43
44 5), observed in this work and in literature³³, could be a consequence of the area of the certain
45
46 devices not containing S vacancies within the gate area probed. Both cases (peaked D_{it} &
47
48 uniform D_{it}) were also reported in Ref 33, showing C-V response of MOS capacitors on semi-
49
50 bulk MoS_2 flakes, indicating that the samples that we report in this work are representative. We
51
52 also suspect that the defect response observed in our devices can potentially originate from other
53
54
55
56
57
58
59
60

1
2
3 impurities and defects present in the flake source ^{44,45} (i.e., the exfoliated MoS₂ crystal), which
4
5 can exhibit equivalent surface density values in the range 1×10^{12} to 1×10^{13} cm⁻². In addition, it is
6
7 possible that the response could originate from defects located in an interfacial transition region
8
9 between the MoS₂ and the HfO₂ ^{49–51} because this methodology can also capture border trap
10
11 response. This is also the subject of on-going studies.
12
13
14

15
16 This work provides a relatively easy fabrication procedure and robust electrical
17
18 characterization methodology to study top-gated metal / high-*k* / TMD devices. The multi-
19
20 frequency C-V response of the structure is consistent with the existence of electrically active
21
22 defects at the interface between high-*k* and MoS₂. By combining with simulation and other
23
24 physical characterization, a route to understand and passivate electrically active interface defects
25
26 in high-*k* gate TMD MOSFETs is possible .
27
28
29
30
31
32
33
34
35
36
37
38
39

40 **Conclusion**

41
42
43 In conclusion, we designed and photolithographically fabricated top-gated FETs on exfoliated,
44
45 few-layer MoS₂ flakes, with an in-situ UV-ozone functionalization treatment and 8nm to 13nm
46
47 ALD HfO₂ dielectrics. Both the transistor performance and the gate-stack interface properties
48
49 were characterized electrically. Based on impedance spectroscopy of the HfO₂/MoS₂ gate stack
50
51 in the MOSFET structure, D_{it} was extracted from the frequency dependence of the C-V response
52
53 using two different methods. The interface state density values were in the range 1×10^{12} to
54
55 1×10^{13} cm⁻² eV⁻¹ for the devices studied, with trapping time constants in the range 1×10^{-5} to
56
57
58
59
60

1
2
3 1×10^{-6} s. One device with 7-L MoS₂ and 13 nm HfO₂ as the gate oxide exhibited a C-V response
4
5 consistent with a D_{it} distribution peaking at a value of 1.2×10^{13} cm⁻² eV⁻¹ at a specific energy in
6
7 the MoS₂ band gap. A second device with 4-L MoS₂ and 8 nm HfO₂ yielded D_{it} values ranged
8
9 from 2×10^{11} cm⁻² eV⁻¹ to 2×10^{13} cm⁻² eV⁻¹ with no peak value of D_{it} observed. The device
10
11 performance and interface properties indicate that the UV-ozone functionalization is promising
12
13 for MoS₂-based devices with high-*k* dielectrics to achieve low leakage, thin and continuous high-
14
15 *k* oxide layers, with interface state density values which allow modulation of the Fermi level at
16
17 the HfO₂/MoS₂ interface. The relatively simple MOSFET test structure, combined with the gate
18
19 to channel C-V response, indicates the existence of specific electrically active HfO₂/MoS₂
20
21 interface defects, and combining these results with simulation and other physical
22
23 characterization methods, will provide an increased understanding of the physical origin of
24
25 defects, as well as a method to monitor the impact of different high-*k* oxides and varying surface
26
27 preparations on the interface state density at high-*k*/MoS₂ interfaces.
28
29
30
31
32
33
34
35
36
37
38
39
40

41 **Supporting Information**

42
43 Proposed equivalent circuits of C-V characterization; Series resistance analysis and full depletion
44
45 of MoS₂ flake; Number of interface defects (N_{it}) extraction from C-V curves; Defects density
46
47 (D_{it}) calculation by high-low frequency method; D_{it} and traps time constant τ_{it} extraction by
48
49 multi-frequency method.
50
51

52 **Corresponding Author**

53
54
55
56
57 *E-mail: chadwin.young@utdallas.edu
58
59
60

Acknowledgment

This work is funded by NSF UNITE US/Ireland R&D Partnership for support under NSF-ECCS-1407765, and Science Foundation Ireland under the US-Ireland R&D Partnership Programme Grant Number SFI/13/US/I2862.

References

- (1) Wang, Q. H.; Kalantar-Zadeh, K.; Kis, A.; Coleman, J. N.; Strano, M. S. Electronics and Optoelectronics of Two-Dimensional Transition Metal Dichalcogenides. *Nat. Nanotechnol.* **2012**, *7*, 699–712.
- (2) Butler, S. Z.; Hollen, S. M.; Cao, L.; Cui, Y.; Gupta, J. A.; Gutiérrez, H. R.; Heinz, T. F.; Hong, S. S.; Huang, J.; Ismach, A. F.; Johnston-Halperin, E.; Kuno, M.; Plashnitsa, V. V.; Robinson, R. D.; Ruoff, R. S.; Salahuddin, S.; Shan, J.; Shi, L.; Spencer, M. G.; Terrones, M.; Windl, W.; Goldberger, J. E. Progress, Challenges, and Opportunities in Two-Dimensional Materials Beyond Graphene. *ACS Nano* **2013**, *7*, 2898–2926.
- (3) Fiori, G.; Bonaccorso, F.; Iannaccone, G.; Palacios, T.; Neumaier, D.; Seabaugh, A.; Banerjee, S. K.; Colombo, L. Electronics Based on Two-Dimensional Materials. *Nat. Nanotechnol.* **2014**, *9*, 768–779.
- (4) Radisavljevic, B.; Kis, A. Mobility Engineering and a Metal-Insulator Transition in Monolayer MoS₂. *Nat. Mater.* **2013**, *12*, 815–820.
- (5) Radisavljevic, B.; Radenovic, A.; Brivio, J.; Giacometti, V.; Kis, A. Single-Layer MoS₂ Transistors. *Nat. Nanotechnol.* **2011**, *6*, 147–150.
- (6) Fuhrer, M. S.; Hone, J. Measurement of Mobility in Dual-Gated MoS₂ Transistors. *Nat. Nanotechnol.* **2013**, *8*, 146–147.
- (7) Kaasbjerg, K.; Thygesen, K. S.; Jacobsen, K. W. Phonon-Limited Mobility in N-Type Single-Layer MoS₂ from First Principles. *Phys. Rev. B - Condens. Matter Mater. Phys.* **2012**, *85*, 1–16.

- 1
2
3 (8) Das, S.; Chen, H. Y.; Penumatcha, A. V.; Appenzeller, J. High Performance Multilayer MoS₂ Transistors
4 with Scandium Contacts. *Nano Lett.* **2013**, *13*, 100–105.
5
6
7
8 (9) Das, S.; Appenzeller, J. Where Does the Current Flow in Two-Dimensional Layered Systems? *Nano Lett.*
9 **2013**, *13*, 3396–3402.
10
11
12 (10) Kim, S.; Konar, A.; Hwang, W.-S.; Lee, J. H.; Lee, J.; Yang, J.; Jung, C.; Kim, H.; Yoo, J.-B.; Choi, J.-Y.;
13 Jin, Y. W.; Lee, S. Y.; Jena, D.; Choi, W.; Kim, K. High-Mobility and Low-Power Thin-Film Transistors
14 Based on Multilayer MoS₂ Crystals. *Nat. Commun.* **2012**, *3*, 1011.
15
16
17 (11) Liu, H.; Ye, P. D. MoS₂ Dual-Gate MOSFET with Atomic-Layer-Deposited Al₂O₃ as Top-Gate
18 Dielectric. *IEEE Electron Device Lett.* **2012**, *33*, 546–548.
19
20
21 (12) Ganatra, R.; Zhang, Q. Few-Layer MoS₂: A Promising Layered Semiconductor. *ACS Nano* **2014**, *8*, 4074–
22 4099.
23
24
25 (13) Ruppert, C.; Aslan, O. B.; Heinz, T. F. Optical Properties and Band Gap of Single- and Few-Layer MoTe₂
26 Crystals. *Nano Lett.* **2014**, *14*, 6231–6236.
27
28
29 (14) Pradhan, N. R.; Rhodes, D.; Feng, S.; Xin, Y.; Memaran, S.; Moon, B. H.; Terrones, H.; Terrones, M.;
30 Balicas, L. Field-Effect Transistors Based on Few-Layered Alpha-MoTe₂. *ACS Nano* **2014**, *8*, 5911–5920.
31
32
33 (15) Cui, Y.; Xin, R.; Yu, Z.; Pan, Y.; Ong, Z.; Wei, X.; Wang, J.; Nan, H.; Ni, Z.; Wu, Y.; Chen, T.; Shi, Y.;
34 Wang, B.; Zhang, G.; Zhang, Y.-W.; Wang, X. High-Performance Monolayer WS₂ Field-Effect Transistors
35 on High- κ Dielectrics. *Adv. Mater.* **2015**, *27*, 5230–5234.
36
37
38 (16) Fang, H.; Chuang, S.; Chang, T. C.; Takei, K.; Takahashi, T.; Javey, A. High-Performance Single Layered
39 WSe₂ P-FETs with Chemically Doped Contacts. *Nano Lett.* **2012**, *12*, 3788–3792.
40
41
42 (17) Liu, W.; Kang, J.; Sarkar, D.; Khatami, Y.; Jena, D.; Banerjee, K. Role of Metal Contacts in Designing
43 High-Performance Monolayer N-Type WSe₂ Field Effect Transistors. *Nano Lett.* **2013**, *13*, 1983–1990.
44
45
46 (18) Zhu, W.; Low, T.; Lee, Y.-H.; Wang, H.; Farmer, D. B.; Kong, J.; Xia, F.; Avouris, P. Electronic Transport
47 and Device Prospects of Monolayer Molybdenum Disulphide Grown by Chemical Vapour Deposition. *Nat.*
48 *Commun.* **2014**, *5*, 3087.
49
50
51
52
53
54
55
56
57
58
59
60

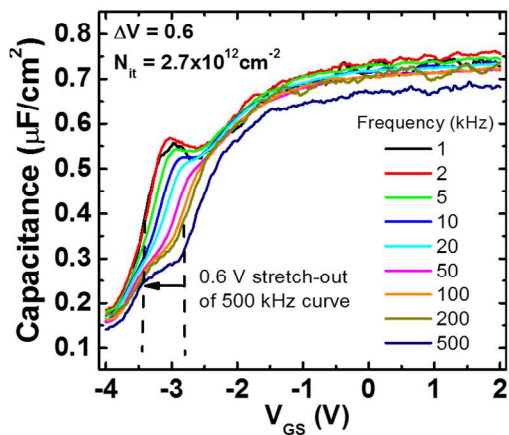
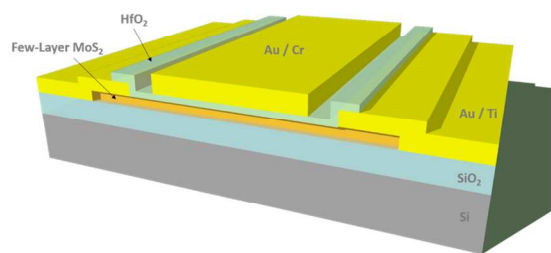
- 1
2
3 (19) Salvatore, G. A.; Münzenrieder, N.; Barraud, C.; Petti, L.; Zysset, C.; Büthe, L.; Ensslin, K.; Tröster, G.
4
5 Fabrication and Transfer of Flexible Few-Layers MoS₂ Thin Film Transistors to Any Arbitrary Substrate.
6
7 *ACS Nano* **2013**, *7*, 8809–8815.
8
9
10 (20) Jena, D.; Konar, A. Enhancement of Carrier Mobility in Semiconductor Nanostructures by Dielectric
11
12 Engineering. *Phys. Rev. Lett.* **2007**, *98*, 1–4.
13
14 (21) McDonnell, S.; Brennan, B.; Azcatl, A.; Lu, N.; Dong, H.; Buie, C.; Kim, J.; Hinkle, C. L.; Kim, M. J.;
15
16 Wallace, R. M. HfO₂ on MoS₂ by Atomic Layer Deposition: Adsorption Mechanisms and Thickness
17
18 Scalability. *ACS Nano* **2013**, *7*, 10354–10361.
19
20
21 (22) Yang, J.; Kim, S.; Choi, W.; Park, S. H.; Jung, Y.; Cho, M.-H.; Kim, H. Improved Growth Behavior of
22
23 Atomic-Layer-Deposited High- K Dielectrics on Multilayer MoS₂ by Oxygen Plasma Pretreatment. *ACS*
24
25 *Appl. Mater. Interfaces* **2013**, *5*, 4739–4744.
26
27
28 (23) Pezeshki, A.; Hosseini Shokouh, S. H.; Raza, S. R. A.; Kim, J. S.; Min, S.-W.; Shackery, I.; Jun, S. C.; Im, S.
29
30 Top and Back Gate Molybdenum Disulfide Transistors Coupled for Logic and Photo-Inverter Operation. *J.*
31
32 *Mater. Chem. C* **2014**, *2*, 8023–8028.
33
34
35 (24) Zou, X.; Wang, J.; Chiu, C.-H.; Wu, Y.; Xiao, X.; Jiang, C.; Wu, W.-W.; Mai, L.; Chen, T.; Li, J.; Ho, J. C.;
36
37 Liao, L. Interface Engineering for High-Performance Top-Gated MoS₂ Field-Effect Transistors. *Adv. Mater.*
38
39 **2014**, *26*, 6255–6261.
40
41
42 (25) Yang, W.; Sun, Q.-Q.; Geng, Y.; Chen, L.; Zhou, P.; Ding, S.-J.; Zhang, D. W. The Integration of Sub-10
43
44 Nm Gate Oxide on MoS₂ with Ultra Low Leakage and Enhanced Mobility. *Sci. Rep.* **2015**, *5*, 11921.
45
46
47 (26) Azcatl, A.; McDonnell, S.; K. C., S.; Peng, X.; Dong, H.; Qin, X.; Addou, R.; Mordi, G. I.; Lu, N.; Kim, J.;
48
49 Kim, M. J.; Cho, K.; Wallace, R. M. MoS₂ Functionalization for Ultra-Thin Atomic Layer Deposited
50
51 Dielectrics. *Appl. Phys. Lett.* **2014**, *104*, 111601.
52
53
54 (27) Azcatl, A.; KC, S.; Peng, X.; Lu, N.; McDonnell, S.; Qin, X.; de Dios, F.; Addou, R.; Kim, J.; Kim, M. J.;
55
56 Cho, K.; Wallace, R. M. HfO₂ on UV-O₃ Exposed Transition Metal Dichalcogenides: Interfacial
57
58 Reactions Study. *2D Mater.* **2015**, *2*, 14004.
59
60

- 1
2
3 (28) Zhao, P.; Vyas, P. B.; McDonnell, S.; Bolshakov-Barrett, P.; Azcatl, A.; Hinkle, C. L.; Hurley, P. K.;
4
5 Wallace, R. M.; Young, C. D. Electrical Characterization of Top-Gated Molybdenum Disulfide Metal-
6
7 oxide-semiconductor Capacitors with High-K Dielectrics. *Microelectron. Eng.* **2015**, *147*, 151–154.
8
9
10 (29) Liu, H.; Si, M.; Deng, Y.; Neal, A. T.; Du, Y.; Najmaei, S.; Ajayan, P. M.; Lou, J.; Ye, P. D. Switching
11
12 Mechanism in Single-Layer Molybdenum Disulfide Transistors: An Insight into Current Flow across
13
14 Schottky Barriers. *ACS Nano* **2014**, *8*, 1031–1038.
15
16 (30) Liu, W.; Sarkar, D.; Kang, J.; Cao, W.; Banerjee, K. Impact of Contact on the Operation and Performance of
17
18 Back-Gated Monolayer MoS₂ Field-Effect-Transistors. *ACS Nano* **2015**, *9*, 7904–7912.
19
20 (31) Park, S.; Kim, S. Y.; Choi, Y.; Kim, M.; Shin, H.; Kim, J.; Choi, W. Interface Properties of Atomic-Layer-
21
22 Deposited Al₂O₃ Thin Films on Ultraviolet/Ozone-Treated Multilayer MoS₂ Crystals. *ACS Appl. Mater.*
23
24 *Interfaces* **2016**, *8*, 11189–11193.
25
26 (32) Mori, T.; Ninomiya, N.; Kubo, T.; Uchida, N.; Watanabe, E.; Tsuya, D.; Moriyama, S.; Tanaka, M.; Ando,
27
28 A. Characterization of Effective Mobility and Its Degradation Mechanism in MoS₂ MOSFETs. *IEEE Trans.*
29
30 *Nanotechnol.* **2016**, *15*, 651–656.
31
32 (33) Takenaka, M.; Ozawa, Y.; Han, J.; Takagi, S. Quantitative Evaluation of Energy Distribution of Interface
33
34 Trap Density at MoS₂ MOS Interfaces by the Terman Method. *IEEE Int. Electron Devices Meet.* **2016**,
35
36 139–142.
37
38 (34) Wang, F.; Stepanov, P.; Gray, M.; Ning Lau, C. Annealing and Transport Studies of Suspended
39
40 Molybdenum Disulfide Devices. *Nanotechnology* **2015**, *26*, 105709.
41
42 (35) Mirabelli, G.; Schmidt, M.; Sheehan, B.; Cherkaoui, K.; Monaghan, S.; Povey, I.; McCarthy, M.; Bell, A. P.;
43
44 Nagle, R.; Crupi, F.; Hurley, P. K.; Duffy, R. Back-Gated Nb-Doped MoS₂ Junctionless Field-Effect-
45
46 Transistors. *AIP Adv.* **2016**, *6*, 25323.
47
48 (36) Cartier, E.; Stathis, J. H. Hot-Electron Induced Passivation of Silicon Dangling Bonds at the Si(111)/SiO₂
49
50 Interface. *Appl. Phys. Lett.* **1996**, *69*, 103.
51
52 (37) O’Sullivan, B. J.; Hurley, P. K.; Leveugle, C.; Das, J. H. Si(100)-SiO₂ Interface Properties Following Rapid
53
54
55
56
57
58
59
60

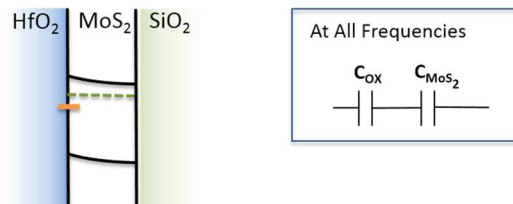
- 1
2
3 Thermal Processing. *J. Appl. Phys.* **2001**, *89*, 3811–3820.
- 4
5
6 (38) Carter, R. J.; Cartier, E.; Kerber, A.; Pantisano, L.; Schram, T.; De Gendt, S.; Heyns, M. Passivation and
7 Interface State Density of SiO₂/HfO₂-Based/polycrystalline-Si Gate Stacks. *Appl. Phys. Lett.*
8 **2003**, *83*, 533.
- 9
10
11
12 (39) Hurley, P. K.; Cherkaoui, K.; O'Connor, E.; Lemme, M. C.; Gottlob, H. D. B.; Schmidt, M.; Hall, S.; Lu, Y.;
13 Buiu, O.; Raeissi, B.; Piscator, J.; Engstrom, O.; Newcomb, S. B. Interface Defects in HfO₂, LaSiO_x, and
14 Gd₂O₃ High-k/Metal–Gate Structures on Silicon. *J. Electrochem. Soc.* **2008**, *155*, G13–G20.
- 15
16
17
18 (40) Bersuker, G.; Park, C. S.; Barnett, J.; Lysaght, P. S.; Kirsch, P. D.; Young, C. D.; Choi, R.; Lee, B. H.;
19 Foran, B.; van Benthem, K.; Pennycook, S. J.; Lenahan, P. M.; Ryan, J. T. The Effect of Interfacial Layer
20 Properties on the Performance of Hf-Based Gate Stack Devices. *J. Appl. Phys.* **2006**, *100*, 94108.
- 21
22
23 (41) Chen, J.; Solomon, R.; Chan, T.-Y.; Ko, P.-K.; Hu, C. A CV Technique for Measuring Thin SOI Film
24 Thickness. *IEEE Electron Device Lett.* **1991**, *12*, 453–455.
- 25
26
27
28 (42) Schroder, D. K. *Semiconductor Material and Device Characterization*; John Wiley & Sons, Inc.: Hoboken,
29 NJ, USA, 2005.
- 30
31
32
33 (43) Choi, K.; Raza, S. R. A.; Lee, H. S.; Jeon, P. J.; Pezeshki, A.; Min, S.-W.; Kim, J. S.; Yoon, W.; Ju, S.-Y.;
34 Lee, K.; Im, S. Trap Density Probing on Top-Gate MoS₂ Nanosheet Field-Effect Transistors by Photo-
35 Excited Charge Collection Spectroscopy. *Nanoscale* **2015**, *7*, 5617–5623.
- 36
37
38
39 (44) Addou, R.; McDonnell, S.; Barrera, D.; Guo, Z.; Azcatl, A.; Wang, J.; Zhu, H.; Hinkle, C. L.; Quevedo-
40 Lopez, M.; Alshareef, H. N.; Colombo, L.; Hsu, J. W. P.; Wallace, R. M. Impurities and Electronic Property
41 Variations of Natural MoS₂ Crystal Surfaces. *ACS Nano* **2015**, *9*, 9124–9133.
- 42
43
44
45 (45) Addou, R.; Colombo, L.; Wallace, R. M. Surface Defects on Natural MoS₂. *ACS Appl. Mater. Interfaces*
46 **2015**, *7*, 11921–11929.
- 47
48
49
50 (46) Qiu, H.; Xu, T.; Wang, Z.; Ren, W.; Nan, H.; Ni, Z.; Chen, Q.; Yuan, S.; Miao, F.; Song, F.; Long, G.; Shi,
51 Y.; Sun, L.; Wang, J.; Wang, X. Hopping Transport through Defect-Induced Localized States in
52 Molybdenum Disulphide. *Nat. Commun.* **2013**, *4*, 1–6.
- 53
54
55
56
57
58
59
60

- 1
2
3 (47) Yu, Z.; Pan, Y.; Shen, Y.; Wang, Z.; Ong, Z.-Y.; Xu, T.; Xin, R.; Pan, L.; Wang, B.; Sun, L.; Wang, J.;
4 Zhang, G.; Zhang, Y. W.; Shi, Y.; Wang, X. Towards Intrinsic Charge Transport in Monolayer
5 Molybdenum Disulfide by Defect and Interface Engineering. *Nat. Commun.* **2014**, *5*, 5290.
6
7
8
9
10 (48) Zhou, W.; Zou, X.; Najmaei, S.; Liu, Z.; Shi, Y.; Kong, J.; Lou, J.; Ajayan, P. M.; Yakobson, B. I.; Idrobo, J.
11 C. Intrinsic Structural Defects in Monolayer Molybdenum Disulfide. *Nano Lett.* **2013**, *13*, 2615–2622.
12
13
14 (49) Dolui, K.; Rungger, I.; Sanvito, S. Origin of the N-Type and P-Type Conductivity of MoS₂ Monolayers on a
15 SiO₂ Substrate. *Phys. Rev. B* **2013**, *87*, 165402.
16
17
18
19 (50) Ghatak, S.; Pal, A. N.; Ghosh, A. Nature of Electronic States in Atomically Thin MoS₂ Field-Effect
20 Transistors. *ACS Nano* **2011**, *5*, 7707–7712.
21
22
23
24 (51) Lu, C.-P.; Li, G.; Mao, J.; Wang, L.-M.; Andrei, E. Y. Bandgap, Mid-Gap States, and Gating Effects in MoS
25 *2. Nano Lett.* **2014**, *14*, 4628–4633.
26
27
28
29
30
31
32
33
34
35
36
37
38
39
40
41
42
43
44
45
46
47
48
49
50
51
52
53
54
55
56
57
58
59
60

Graphic for Table of Contents (TOC)



(i) $V_{\text{GS}} > -2.8$ V in depletion region



(ii) $-3.4 \text{ V} < V_{\text{GS}} < -2.8$ V (E_{F} pinned)

